RSC Advances

ROYAL SOCIETY OF CHEMISTRY

www.rsc.org/advances

Journal Name

RSCPublishing

COMMUNICATION

Crystalline $Li_3V_6O_{16}$ Rods as High-Capacity Anode Materials for Aqueous Rechargeable Lithium Batteries (ARLB)

Cite this: DOI: 10.1039/x0xx00000x

Received 00th January 2012,
Accepted 00th January 2012

DOI: 10.1039/x0xx00000x

www.rsc.org/

Vivek Sahadevan Nair,[a,b,§] Sivaramapanicker Sreejith,[c,§] Parijat Borah,[c] Steffen Hartung,[d,e] Nicolas Bucher,[d,e] Yanli Zhao[a,c] and Srinivasan Madhavi[a,b,d]

We report the preparation of highly crystalline $Li_3V_6O_{16}$ rods (LVO-1 rods) and their use as anode materials for the first time in aqueous rechargeable lithium ion batteries (ARLB). A half-cell ARLB with LVO-1 as anode materials delivers higher initial capacity of >120 $mAhg^{-1}$ at high current rate and higher round trip efficiency of 52% at the end of 100 cycles at a current density of 500mA.g^{-1}. ARLB with LVO-1 rods as anodes exhibited excellent rate and cycling performances.

Most of the portable electronic devices nowadays uses lithium ion battery as their major source of energy storage.[1-6] Major problems related to lithium ion batteries include usage of flammable organic electrolyte, presence of highly reactive and inflammable electrode components and ruggedness in its usage.[7,8,9] Also, leak in packaging of a lithium ion battery can render the battery to combust or make it incompetent to perform. Most of the major fires and accidents in automobile and aircraft engines are due to lithium ion batteries.[10] In recent days, three Tesla Motors Model S electric cars have caught fire after their lithium-ion battery packs were damaged raising doubts in the minds of the public regarding safety and terming electric vehicles as a fire hazard.[11] Hence, it would be even difficult to imagine to use these lithium ion batteries in wearable sports application, where these batteries comes in direct contact with the human body.

Li et. al.,[12] reported a new possibility for energy storage i.e., aqueous rechargeable lithium ion battery (ARLB) which was a safer alternative and could prove to be competent enough to match the performance of current lithium ion batteries. As ARLB systems use water as the electrolyte medium, leakage in an ARLB package would most probably not result into fire or reduce the performance of the battery, thus rendering it useful for many applications like electric vehicles, large scale grid based energy storage and more importantly in portable and wearable electronics.[13,14] However, owing to the complicated reactions possibilities in a typical ARLB, a rational selection of the electrode materials in ARLB remains challenging.[13-16] Only electrodes which fall within the oxidation and reduction potential of water, avoiding the release of oxygen or hydrogen during the battery charge-discharge process can be used for any practical application. Hence, the overall voltage and therefore energy density of the battery is limited due to the nature of the electrode that operates in an aqueous system.[17] For making ARLBs equally competent to lithium ion battery, increase in its overall energy density is detrimental. In this context design of new electrode materials for ARLBs with higher rate of performance is of great importance.

Generally in ARLB systems, $LiMn_2O_4$ has been studied extensively with an operating voltage of 0-1.0 V vs SCE (Standard calomel electrode).[18] Commonly used anode materials like TiP_2O_7, $LiTi_2(PO4)_3$ and LiV_3O_8 in ARLBs gives a discharge capacity of 100$mAhg^{-1}$, 80mAh g^{-1} and 40$mAhg^{-1}$ respectively with a cycle life efficiency of only ~35% (25 cycles), ~38%(25 cycles) and 53.5%(100 cycles) respectively.[15,16,19] Vanadium oxides and bronzes are sought out to be one of the best materials for large scale energy storage due to their tunable structural flexibility, high discharge capacity, abundance and low cost amongst the numerous other transition metal oxides.[20-24] Various vanadium oxide has been studied for ARLB applications like LiV_2O_5, LiV_3O_8, VO_2 (B) but their practical capacities are 47mAh g^{-1}, 45mAh g^{-1} and 100mAh g^{-1} respectively and their capacities fall down to approximately <50% at the end of 100 cycles.[25] In the case of LiV_3O_8, its layers are made up of VO_6 octahedra and VO_5 tetrahedra which are held together by immobile lithium ions situated at the interlayer octahedral sites. In aqueous electrolyte, LiV_3O_8 shows a capacity of <45 $mAhg^{-1}$ and a poor cycling performance due to vanadium dissolution followed by collapse of its crystal structure. To improve the overall efficiency and usability of ARLBs, development of a potential anode material with sufficiently high capacity, higher voltage window and increased cycle life stability is essential.

Here, we report a facile hydrothermal preparation of $Li_3V_6O_{16}$ rods (hereafter referred as LVO-1 rods) with high crystallinity and demonstrated its application as anode materials in ARLB. In this work, we report a novel $Li_3V_6O_{16}$ anode material with wide operating potential -1.1- 0 V vs SCE that can be used as an anode to fabricate a 2V ARLB system with cathode materials like $LiMn_2O_4$, $LiNiO_2$, $LiCoO_2$, $LiFePO_4$, thereby improving the overall energy

density of the ARLB system significantly. In a typical experiment a mixture of Lithium acetate ($CH_3COOLi•2H_2O$) and vanadium pentoxide (V_2O_5) in 25 mL distilled deionized water in 1:1.2 molar ratio respectively was prepared. The resulting solution was mixed thoroughly by stirring until it turns red with pH 9.0. The solution was neutralized and allowed to undergo hydrothermal process in Teflon-lined stainless steel autoclave for 48 h at 200ºC. The product was collected by centrifugation followed by repeated washing in deionized water and ethanol in order to remove any possible ionic remnants and dried in vacuum overnight at 105ºC. The sample was then calcinated at 400ºC and ground in order to obtain the highly crystalline LVO-1.

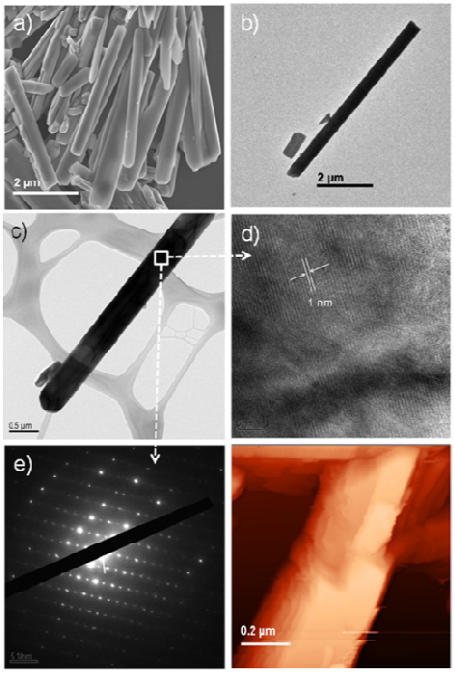

Fig. 1 LVO-1: a) FE-SEM image b) TEM image (low resolution), c) HR-TEM image d) lattice fringe obtained from selected area. e) SAED pattern and f) AFM image.

The readily prepared LVO-1 was then characterized using field emission scanning electron microscope (FE-SEM) high resolution transmission electron microscope (HR-TEM) and atomic force microscope (AFM). FE-SEM images (Figure 1 a) of LVO-1 shows extended rod-like morphology with aspect ratio ~20 (average diameter of ~0.5µm and length ≤5µm). TEM is shown in Figure 1b shows clear formation of extended rods. From HR-TEM (Figure 1c) the obtained lattice fringe pattern (Figure 1d) and selected area electron diffraction (Figure 1e) of LVO-1 rods reveals the presence of several layers of lamellar crystals which leads to the formation of extended rod morphology. LVO-1 has a higher surface area thereby rendering it useful for faster charge-discharge in batteries. Similarly, AFM image (Figure 1f) also shows the rod like morphology of LVO-1 as consistent with the images observed in FE-SEM and TEM. The powder XRD patterns (Figure S1) were collected to elucidate the crystal structure of LVO-1 and evaluated using the Rietveld refinement method. The XRD patterns (Figure 2a) can be fully indexed to the crystal structure of $Li_3V_6O_{16}$ ($P12_1/m1$, PDF 4-0417) *via* Rietveld refinement(R factor <0.06), without the presence of any impurity peaks. The XRD data shown in Figure 2 for LVO-1 can be reasonably indexed to the observed selected area diffraction pattern in Figure 1e.

The X-ray Photoelectron Spectroscopy (XPS) survey spectrum (Supporting Information, Figure S2) reveals the presence of Lithium, Vanadium and Oxygen without any impurities. The high resolution spectrum of $V2p_{3/2}$ and $V2p_{1/2}$ centered at 516.1 and 523.6 eV respectively indicates the presence of V^{5+} species (Figure S3a). Similarly for the Li 1s region, the core level is as 54.85 eV with the dominant Li signal assigned to Li^+ (Figure S3b). Hence we prove the monoclinic nature of $Li_3V_6O_{16}$ with no evident impurities detected.

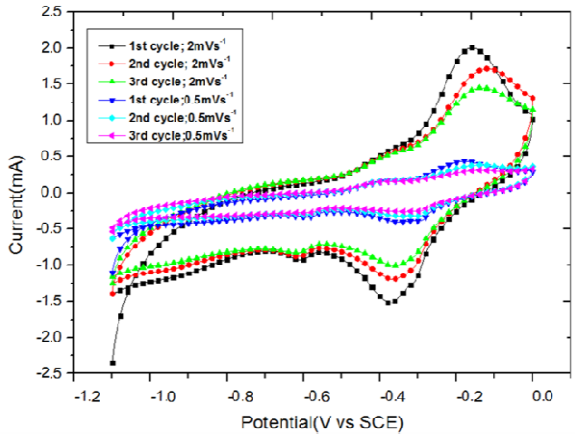

Fig. 2 Cyclic voltammograms of LVO-1 as anode in three electron configuration (vs SCE) from -1.2 to 0V at scan rate of $0.5mVs^{-1}$ and $2mVs^{-1}$

To elucidate the electrochemical processes of the ARLB, cyclic voltammetry (CV) and galvanostatic charge/discharge of the half cells were carried out in a three-electrode configuration. 3M lithium nitrate ($LiNO_3$) aqueous solution was used as electrolyte, with platinum foil and a SCE as the counter and reference electrodes respectively. Voltage range was computer-controlled using potentiostat (Solartron, 1470E) at room temperature, in the voltage range of 0 to 1.9V *vs.* SCE. In order to investigate the phase transformations occurring during the electrochemical processes cyclic voltammetric tests (Figure 2) of the LVO-1 rods as anode was carried out in three-electrode configuration within the potential range of -1.1 to 0.0V at a scan rate of $0.5mVs^{-1}$ and $2mVs^{-1}$. In the anodic CV of LVO-1, two main reduction peaks can be observed at -0.4V and -0.6V while a faint reduction peak can be observed at -0.3V *vs.* SCE and two main oxidation peaks at -0.425V and -0.275V *vs.* SCE respectively. These peaks indicate lithium insertion (reduction)/de-insertion (oxidation) processes occurring during electrochemical charging/discharging.

We then evaluated the electrochemical charge/discharge performance of LVO-1 as anode as shown in Figure 3a using three electrode configuration at a current density of 0.5 $mAhg^{-1}$. LVO-1 as anode gave an initial charge capacity of 110 $mAhg^{-1}$ and discharge capacity of 120 $mAhg^{-1}$. Apparently, all the specific capacity values are calculated with respect to the mass of the active material. LVO-1 displays a slightly higher anode capacity at a higher negative voltage window compared to other commonly used anode materials like TiP_2O_7, $LiT_2(PO_4)_3$ and LiV_3O_8 in ARLBs. The absence of a flat discharge plateau can be attributed to the multi-lithium ion intercalation/de-intercalation process.[25] The cyclic performance of LVO-1 active materials was further evaluated by prolonged cycling, up to 100 cycles, at 0.5 Ag^{-1} as shown in Figure 3b. Figure 3c shows the cyclic stability of LVO-1 for 10 cycles each at varying current densities. The discharge capacity at the end of 100 cycles for LVO-1

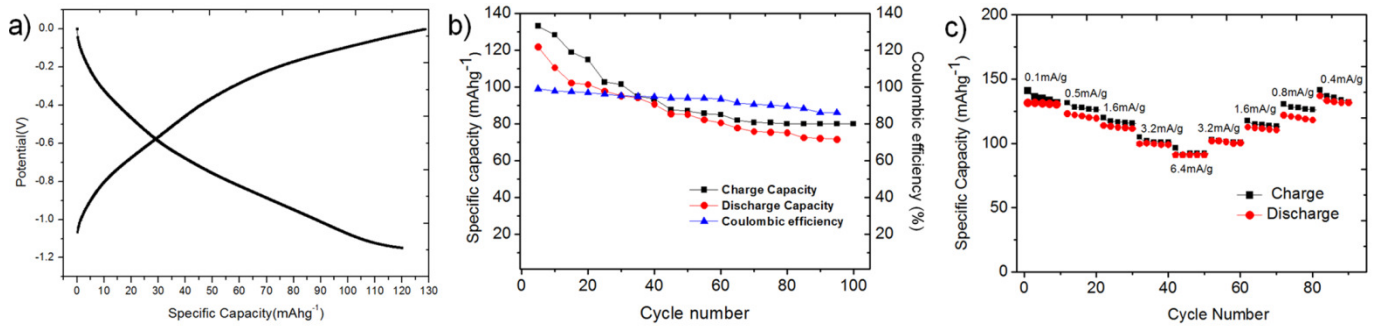

Fig. 3 a) Galvanostatic discharge/charge profiles of LVO-1 in 3M $LiNO_3$ aqueous solution, in three electrode configuration (*vs.* SCE) from -1.2 to 0V, at current density of 0.5 mAg^{-1}. b) Cycling performance and columbic efficiency of LVO-1 as anode in ARLB at a current density of 0.5 mAg^{-1} and c) Rate performance of LVO-1 for 10 cycles each at current densities of 0.1mA/g, 0.5mA/g, 1.6mA/g, 3.2mA/g and 6.4mA/g in the cut-off voltage window -1.2 to 0V *vs.* SCE.

was 62.5mAh g^{-1} with ~52% equivalent to retention of initial capacity. Hence, the cyclic stability of LVO-1 can be attributed to the higher surface area and higher crystallinity (larger crystal size) as evident from the TEM, AFM (Figure 1) and XRD (Figure S1).

Increase in the aspect ratio of the LVO-1 rods leads to higher electro-active surface area and reduced ion diffusion path. This, in turn, improves the mobility of lithium ions within the active material, enabling a larger number of lithium ions to intercalate into the active electrode material and occupy the vacant tetrahedral and octahedral sites in the crystal structure of LVO-1. Crystal structure, electrode porosity and composition of the materials also play a very important role in imparting high rate capabilities in anode materials.[26] The pseudo-layered crystal structure of LVO-1 facilitates the lithium insertion/de-insertion into and from the layers via the diffusion, while presence of lithium ions (Li^+) residing in the octahedral sites[27-31] aids in maintaining the pseudo-layered structure, by supporting the $V_6O_{16}^-$ puckered layers, during the electrochemical lithiation/de-lithiation processes, resulting in excellent electrochemical performance in terms of rate capability and cyclic stability.[24,32] Good Columbic efficiency in the range of 99-86% was achieved over the cycles from 1-100 at a high current density of 0.5Ag^{-1} (Figure 3b).

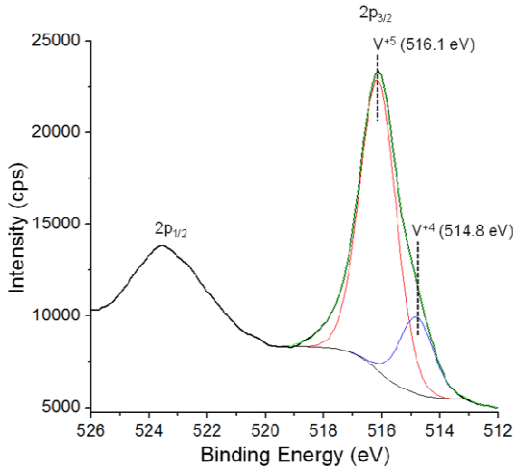

Fig. 4 High-resolution XPS spectra of LVO-1 at the V2P region after charge/discharge showing existence of vanadium in the $V^{+5/+4}$ oxidation states.

After the electrochemical charge/discharge performance of LVO-1 as anode, the electrode was examined again by XPS (Figure 4). In the high resolution XPS spectrum of V2p region, new peaks in both $V2p_{3/2}$ and $V2p_{1/2}$ orbital can be observed along with the peaks correspond to V^{5+} species. These new peaks can be attributed to V^{4+} species which can be believed to be generated during the charging process. Further, since the overall capacity of a material like LVO-1 can have different relative contributions of surface capacitive and diffusion controlled bulk intercalation processes which can be measured using electrochemical methods.

$Li_3V_6O_{16}$ has a pseudo-layered structure where the layers are held together by the two lithium ions present in the octahedral pockets of the structure. We differentiate the modes of charge storage mechanisms in $Li_3V_6O_{16}$ nanowires i.e. surface-capacitance and bulk lithium intercalation by fitting the voltammetric currents at various sweep rates (Figure 5a) to appropriate power law relationships given by equation 3 derived from equations 1 and 2 (See Supporting Information). Total charge storage depends exclusively on both capacitive and lithium intercalation processes. From Figure 5b surface capacitance contribution of LVO-1 was computed to be ~22.22% and intercalation capacity of ~77.83% at 4mVs^{-1} while at 0.5mVs^{-1} respectively (Figure S4). Similarly, the surface capacitance contribution substantially decreased to ~9.17% with corresponding increase in intercalation capacity to ~90.82% (Figure 5). Usually surface-capacitance based energy storage behavior helps in stable operation at higher current densities (i.e. faster charge/discharge kinetics) thereby better power density while Li-ion intercalation based energy storage mechanism helps in higher capacity and hence increased energy density. Knowledge of the charge storage mechanism is necessary to tune the two faradaic based charge storage mechanisms which plays crucial role to obtain a battery with desired functionality for different application. Tuning morphology, size of the material and replacement of the intercalating ion are some of the strategies that can be used to tune the charge storage mechanism.

Conclusions

In conclusion, here we have demonstrated the successful synthesis of LVO-1 having rod like morphology by a facile hydrothermal method, followed by subsequent heat-treatment at 400°C. Characterization via FE-SEM, TEM, AFM revealed the formation of rod-like structures with high aspect ratio >20. X-ray diffraction confirmed the formation of 100% crystalline phase pure synthetic lithium vanadate bronze $Li_3V_6O_{16}$ (LVO-1). The

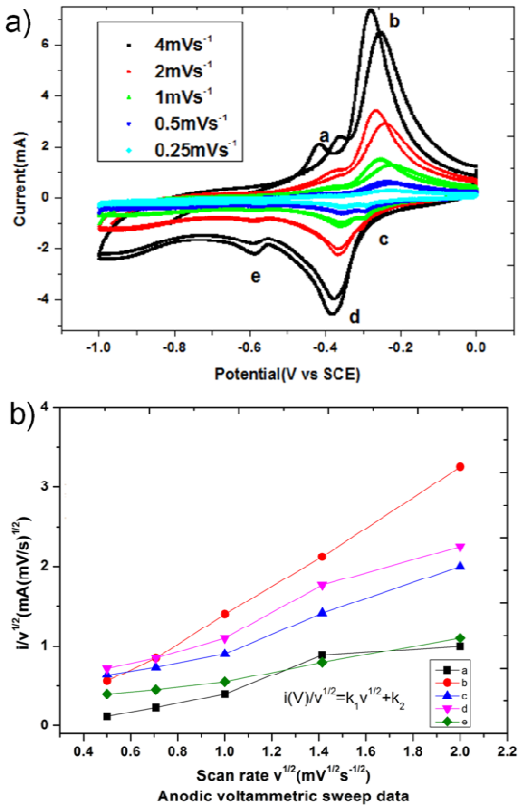

Fig. 5 a) Cyclic voltammetric response of LVO-1 rods at sweep rates of 4mVs^{-1} (a), 2mVs^{-1} (b), 1mVs^{-1} (c), 0.5mVs^{-1} (d) and 0.25mVs^{-1} (e) respectively. b) Charge storage mechanism using inverse power law with peak currents corresponding to cycles a, b, c, d & e as shown in Fig 5a.

application of LVO-1 as anode material in an aqueous lithium ion battery (ARLB) was demonstrated and the electrochemical properties were studied via cyclic voltammetry and galvanostatic charge/ discharge. High initial capacity of >120mAhg^{-1} at high current rate was achieved. Upon cycling to 100 cycles, ~52% of initial capacity was retained, exhibiting the superior rate performance and cycling stability of LVO. More importantly, it can be deduced that the layered structure of LVO, coupled with the presence of three lithium ions, resulted in a stable structure, enabling the ease of lithium intercalation/deintercalation, leading to future applications of LVO-1 as potential electrode material for aqueous lithium ion batteries. The charge storage mechanism was studied by performing cyclic voltammetric experiments with LVO-1 as anode at various voltage sweep rates, from which we observed a dominant bulk lithium ion intercalation based charge storage in LVO-1 compared to the intercalation and double-layer capacitance based charge storage.[33] Further studies on LVO-1 could target to improve its volumetric energy density by enhancing the diffusion controlled lithium insertion along with the surface-capacitive charging by tailoring different nanoarchitectures and alkali-metal ion replacement is ongoing.

Notes and references

[a] School of Materials Science and Engineering, Nanyang Technological University, 50 Nanyang Avenue, 639798, Singapore. Email: madhavi@ntu.edu.sg

[b] Institute for Sports Research, Nanyang Technological University, 50 Nanyang Avenue, 639798, Singapore.

[c] Division of Chemistry and Biological Chemistry, School of Physical and Mathematical Sciences, Nanyang Technological University, 21 Nanyang Link, 637371, Singapore.

[d] TUM-CREATE, 1-Create Way, 138602, Singapore.

[e] Technische Universität München, 85748, Garching, Germany.

§ These authors contributed equally to this work.

† We acknowledge Timcal for providing Super P-Li Carbon black. These authors are grateful to The Nanyang Technological University and Ministry of Education, Singapore for financial support.

Electronic Supplementary Information (ESI) available: [details of any supplementary information available should be included here]. See DOI: 10.1039/c000000x/

1 M. Winter and R. J. Brodd, *Chem. Rev.* 2004, **104**, 4245-4270.
2 V. Etacheri, R. Marom, R. Elazari, G. Salitra and D. Aurbach, *Energy Environ. Sci.*, 2011, **4**, 3243.
3 *Advanced in Lithium-ion Batteries* (Eds: W. van Schalkwijk, B. Scrosati), Kluwer Academic/Plenum, New York, 2002.
4 M. S. Whittingham, *Chem. Rev.* 2004, **104**, 4271-4302.
5 *Lithium Batteries Science and Technology* (Eds.: G.-A. Nazri, G. Pistoia), Kluwer Academic/Plenum, Boston, 2004.
6 B. Dunn, H. Kamath and J. –M. Tarascon, *Science*, 2011, **334**, 928-935.
7 T. M. Bandhauer, S. Garimella and T. F. Fuller, *J. Electrochem. Soc.* 2011, **158**, R1-R25.
8 G. L. Soloveichik, *Annu. Rev. Chem. Biomol. Eng.* 2011, **2**, 503-527.
9 Z. Yang, J. Zhang, M. C. W. Kinter-Meyer, X. Liu, D. Choi, J. P. Lemmon and J. Liu, *Chem. Rev.* 2011, **111**, 3577-3613.
10 http://www.bbc.co.uk/news/business-21054089
11 http://www.technologyreview.com/news/521976/are-electric-vehicles-a-fire-hazard/
12 W. Li, J. R. Dahn and D. S. Wainwright, *Science*, 1994, **264**, 1115-1118.
13 W. Tang, Y. Zhu, Y. Hou, L. Liu, Y. Wu, K. P. Loh, H. Zhang and K. Zhu, *Energy Environ. Sci.*, 2013, **6**, 2093-2104.
14 G. Wang, L. Fu, N. Zhao, L. Yang, Y. Wu and H. Wu, *Angew. Chem. Int. Ed.* 2006, **46**, 295-297.
15 H. Wang, K. Huang, Y. Zeng, S. Yang and L. Chen, *Electrochim Acta*, 2007, **52**, 3280-3285.
16 X. -H. Liu, T. Saito, T Doi, S. Okada and J. -I. Yamaki, *J. Power Sources*, 2009, **189**, 706-710.
17 H. Majunatha, G. S. Suresh and T. V. Venkatesha, *J. Solid State Electrochem.* 2011, **15,** 431-445.
18 J. Y. Luo, W. J. Cui, P. He and Y. Y. Xia, *Nat. Chem.* 2010, **2**, 760-765.
19 J. Köhler, H. Makihara, H. Uegaito, H. Inoue and M. Toki, *Electrochim. Acta*, 2000**, 46**, 59-65.
20 J. Jiang, Z. Wang and L. Chen, *J. Phys. Chem. C*, 2007, **111**, 10707-10711.
21 H. Liu, Y. Wang, L. Li, K. Wang, Y. Wang and H. Zhou, *J. Power Sources*, 2009, **192**, 668-673.
22 H. Liu, Y. Wang, L. Li, K. Wang, E. Hosono and H. Zhou, *J. Mater. Chem.*, 2009, **19**, 7885-7891.

23 N. A. Chernova, M. Roppolo, A. C. Dillon and M. S. Whittingham, *J. Mater. Chem.*, 2009, **19**, 2526-2552.
24 G. Q. Liu, C. L. Zeng and K. Yang, *Electrochim. Acta*, 2002, **47**, 3239-3243.
25 D. Zhou, S. Liu, H. Wang and G. Yan, *J. Power Sources*, 2013, **227**, 111-117.
26 C. Fongy, A.-C. Gaillot, S. Jouanneau, D. Guyomard and B. Lestriez, *J. Electrochem. Soc*., 2010, **157**, A885-A891.
27 J. Yu, J. C. Yu, W. Ho, L. Wu and X. Wang, *J. Am. Chem. Soc.*, 2004, **126**, 3422-3423.
28 W. Avansi Jr, C. Ribeiro, E. R. Leite and V. R. Mastelaro, *Mater. Chem. Phys.*, 2011, **127**, 56-61.
29 J. Kawakita, M. Majima, T. Miura and T. Kishi, *J. Power Sources*, 1997, **66**, 135-139.
30 Y. Liu, X. Zhou and Y. Guo, *Electrochim. Acta*, 2009, **54**, 3184-3190.
31 H. Wang, W. Wang, Y. Ren, K. Huang and S. Liu, *J. Power Sources*, 2012, **199**, 263-269.
32 H. Wang, K. Huang, S. Liu, C. Huang, W. Wang and Y. Ren, *J. Power Sources*, 2011, **196**, 788-792.
33 S. Liu, S. H. ye, C. Z. Li, G.. L. Pan and X. P. Gao, *J. Electrochem. Soc.*, 2011, **158**, A1490-A1497.